A study on efficiency of magnetic levitation trains using linear induction motor by slip pattern

1st Hyunuk Seo
Department of Robotics & Mechatronics
Korea Institute of Machinery & Materials
Daejeon, Korea
shu@kimm.re.kr

2nd Jaewon Lim
Department of AI Machinery
Korea Institute of Machinery & Materials
Daejeon, Korea
einses@kimm.re.kr

3rd Sang Uk Park
Department of Electrical Eng
Konkuk University
Seoul, Korea
shyman01@konkuk.ac.kr

4th Hyung-Soo Mok
Department of Electrical Eng
Konkuk University
Seoul, Korea
hsmok@konkuk.ac.kr

***Abstract*—Linear induction motors used in magnetic levitation (maglev) trains use a higher constant slip frequency operating scheme than rotary motors to meet thrust and normal force requirements. Thus, the constant slip frequency is used in all operation conditions, which reduces the efficiency of the propulsion system. In this paper, a varying slip frequency control is proposed for increasing the propulsion efficiency within the limit of vertical force disturbance. The operation pattern of the actual train is defined by the route travel plan, which is adopted in simulation. The proposed varying slip frequency control pattern is verified by the actual maglev train test. With the proposed algorithm, efficiency consumption is improved not only in the propulsion system but the total power in the maglev train operation.**

***Index Terms*—Linear induction motor, Maglev train, Vector Control**

I. Introduction

Owing to the rapid industrialization of modern society, the demand for fast and clean railway transportation is increasing due to the increased travel demands of commuters. Magnetic levitation (maglev) systems have many advantages over conventional wheel-on-rail systems, namely, better ride quality, lower exposure to dust, and lower management costs. In particular, the maglev trains Fig. 1 are known to have lower maintenance costs than conventional train systems owing to their mechanical non-contact characteristics. However, it has been observed that its energy consumption is higher than wheel-on-rail systems [1].

The major components of maglev trains can be divided into the propulsion system and levitation system, as in Fig. 2. Most of the energy consumption on a maglev train occurs in these systems. As a propulsion system for maglev trains, the high-speed trains mainly use linear synchronous motors (LSMs), and the low-speed trains use linear induction motors (LIMs). In the case of an urban maglev train, the operation is in the relatively low-speed range, so it is common to use an LIM to lower construction costs. The maglev system of a high-speed train uses a superconducting magnet or an electromagnet

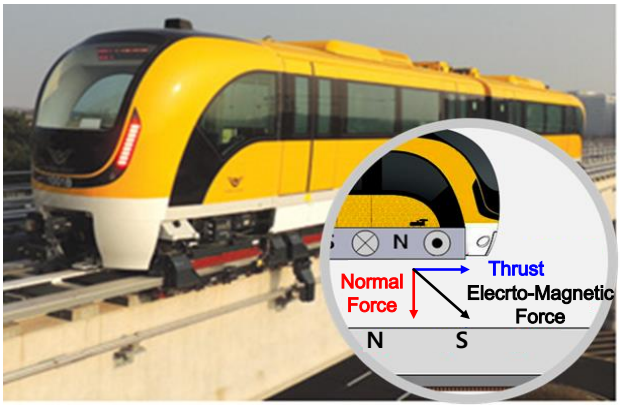

Fig. 1. Maglev train in KOREA

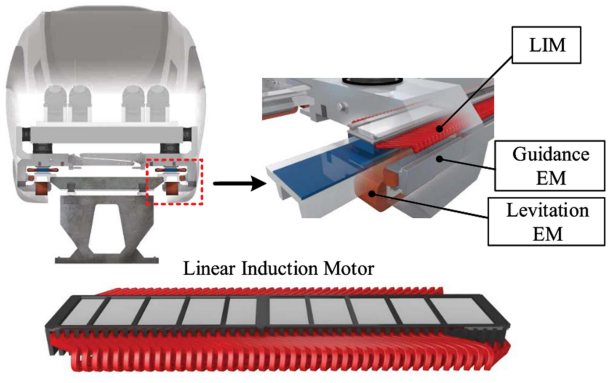

Fig. 2. Traction system of maglev train

978-1-7281-0395-2/19/$31.00 ©2019 IEEE

integrated with the LSM. In the case of low-speed trains, it is common to use attractive electromagnets as the levitation system.

Unlike a rotating machine, a linear motor generates a vertical force in a direction orthogonal to the traveling direction [2]. This characteristic causes disturbance in the levitation system [3]. The levitation system should therefore be designed to consider not only the force that lifts the weight of the vehicle but also the normal force generated by the propulsion system. A low vertical force is required in the propulsion system, but it is also very important to reduce the disturbance of the maglev system by generating a constant vertical disturbance. Therefore, in the previous version of the maglev control, the variation of the vertical force by the LIM was minimized through constant slip frequency control, and the stability of the maglev system was achieved. However, this algorithm does not allow high efficiency driving of the propulsion system.

The energy ratio of the levitation system to the propulsion system vary between 0.1 and 0.4 according to the operating conditions, which are determined by acceleration, coasting, and deceleration [4] of the train. Therefore, in order to increase the energy efficiency of the maglev train, it is essential to improve the efficiency of the propulsion system.

In this study, the optimal slip frequency is extracted by analyzing and testing the propulsion and levitation systems on a low-speed maglev train in Korea. In order to operate the LIM of the train with optimum efficiency, the slip is changed according to the current and speed. The proposed propulsion algorithm is verified by actual testing on a train, and higher energy efficiency was achieved through the tests.

II. Propulsion System

A. Normal Force and Constant Slip Frequency Control

When electric motors generate thrust or torque, the electromagnetic force is generated in the traveling direction and attraction force in the vertical direction. For a rotary induction motor (IM), the attractive force between the stator and the rotor cancel each other because it is symmetrical about the axis. Thus, for a low slip frequency range or a varying slip frequency operation, the attraction force can be neglected. Even for a general LIM, the vertical force is stably supported by the linear guide; thus, it affects only the frictional force. Unlike other systems, the normal force in the maglev train should be carefully examined because this disturbance can cause levitation failure or abnormal operation. During the maximum thrust control, the vertical force of the propulsion system can be expressed as a function of the slip frequency and must be within an allowable range to reduce the disturbance of the levitation system.

TABLE I
Design Specifications of LIM for Low-Speed Maglev Train

LIM		Levitation Electromagnet	
Parameter	**Value**	**Parameter**	**Value**
Length	1785 mm	Length	2600 mm
Number of pole	8	Number of yokes/poles	4
Number of slots	53	Number of coils/poles	2
Turns/coil	5	Turns/coil	193
Al plate thickness	5 mm	Pole width	32 mm
Airgap	11 mm	Airgap	8 mm
Required thrust	60.4 kN/train	Rated lift force	33 kN
Maximum speed	110 km/h		

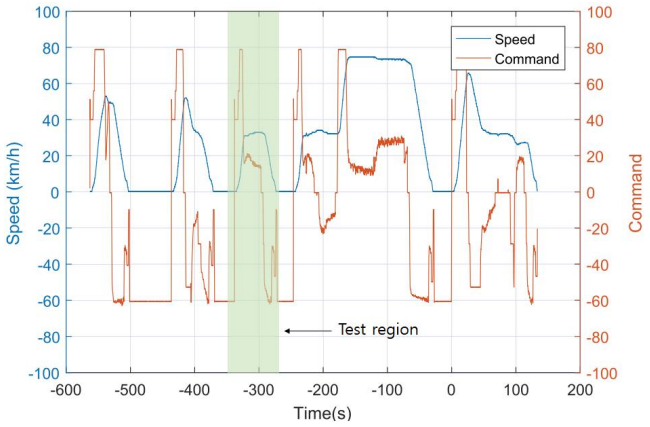

Fig. 3. Speed and thrust command of ECOBEE [4].

In a rotating IM, a dq axis-based vector control is commonly used. However, in general vector control, the slip frequency varies according to the torque command, which induces a levitation system disturbance. The variation of the small slip frequency produces a large vertical force variation, particularly when the propulsion is operating in the low speed range. Therefore, the LIM uses scalar control with the slip frequency as the control variable; further, the vertical force limiting characteristic of the constant slip frequency control is suitable for the stable driving in the low speed region [3].

B. Propulsion System in Low Speed Maglev

The basic performance parameters of an LIM are rated speed, maximum speed, and maximum thrust. The major design parameters of the LIM are listed in Table I. At the design stage, the maximum thrust is determined by considering the emergency operation, and the maximum speed is determined considering the maximum performance of the train. However, in practical situations, the maximum thrust operation is not frequently used except during emergencies; further, the maximum speed operation is not often used because of the route condition.

The distribution of the frequently used area according to the thrust command and speed is shown in Fig. 3. For operation in the entire route, only the powering period was analyzed and the standstill levitation is excluded. The propulsion command was controlled by automatic train operation (ATO). The full-notch powering operation time is only 20%, because the maglev trains have excellent acceleration and coasting performance. Eighty percent of the thrust command is under the half-notch operation. In the low thrust command area, the most frequent speed ranges are 30 km/h and 70 km/h, because they are the primary coasting regions along this route.

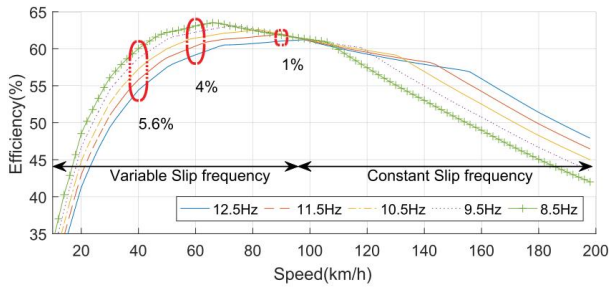

Fig. 4. Efficiency with variable slip frequency [4]

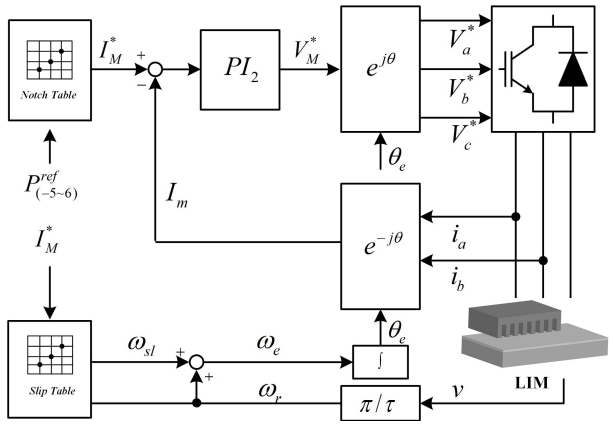

Fig. 5. Propulsion control algorithm of maglev trains

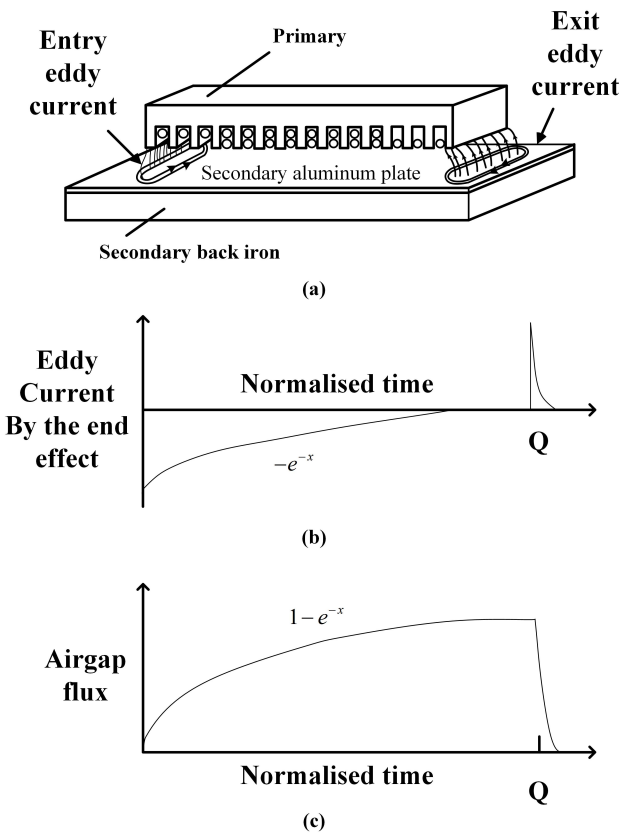

Fig. 6. LIM (a) Eddy current generation at the entry and exit of the air gap (b) Eddy current density profile along the length of the LIM (c) Air gap flux profile [6]

C. Variable Slip Frequency Control

To improve the propulsion efficiency of the maglev train, the variable slip frequency is controlled. This is done carefully because it causes fluctuations in the disturbances of the levitation system. The proposed algorithm varies the slip frequency to realize high efficiency of the propulsion system; however, it limits the range of the slip frequency. Then, the vertical force can be maintained within the range of the maximum vertical force disturbance that was analyzed during the constant slip frequency control.

The efficiency for the variable slip frequency is shown in Fig. 4. According to the previous research, the proposed constant slip frequency control is advantageous to achieve high propulsion efficiency at high speed; low slip frequency for low speed is favorable to achieve high propulsion efficiency [4].

D. Traction Algorithm for Variable Slip Frequency Control

Fig. 5 is a LIM propulsion algorithm for maglev trains [5]. The current command generated according to the driving pattern and route information of the train is compared with the current supplied to the motor; the PI control is performed to generate the voltage command. This command uses the electric angular frequency by adding the slip frequency obtained from the vehicle speed and current command and the angular frequency obtained by the current vehicle position.

The conventional algorithm uses a constant slip frequency for all currents and speeds. This is because LIMs generate high vertical forces when using low slip as in a rotating electric motor. However, because the energy ratio of the propulsion system is higher than that of the levitation system during acceleration/deceleration, increasing the efficiency of the propulsion can help achieve higher efficiency from the viewpoint of the total energy.

In this algorithm, the constant slip of 12.5 Hz was linearly varied to 6 Hz for a low current command considering the test condition and specification of the levitation system.

III. Mathematical Model of LIM for Maglev Train

In the dynamic analysis of electrical machines, the mathematical model is used to approximate the dynamic motion of the electric device to a high level, so that the experimental results can be accurately predicted. This section outlines a mathematical model of LIMs for the maglev train.

A. End Effect of LIM

Fig. 6. shows a LIM. Both the generation and decay of fields result in an eddy current in the secondary sheet. The eddy current in the entry increases rapidly to mirror the magnetizing current, nullifying the air gap flux at the entry. On the other hand, the eddy current at the exit weaken the field, which makes the dragging force of the primary core.

The density profile of the eddy current along the length of LIM is similar to that depicted in Fig. 6(b) [7]. Hence, the resulting magnetomotive force (MMF), and thereby the air gap flux, resemble those in Fig. 6(c). Duncan introduced a dimensionless factor Q, which is defined as

$$Q \triangleq \frac{T_1}{T_2} = \frac{l/v_2}{L_2/R_2} \tag{1}$$

where l, v_2, L_1 and R_2 are the motor length, velocity,secondary self-inductance, and secondary resistance, respectively [7]. T_1 is the time for the primary core to traverse a point in the rail, and $T_2 = L_2/R_2$ is the time constant of the secondary circuit. Q represents the motor length for a given speed v_2 but normalized by the secondary time constant. On this basis, the motor length is infinite at zero speed and will decrease as the speed increases. Note that if we scale the position x' by

$$X \equiv \frac{x'/v_y}{L_y/R_y} \tag{2}$$

the motor air gap resides in the interval, $[0, Q]$, where the amplitudes (envelope) of the eddy and magnetizing currents are assumed to be given by $-I_m e^{-x}, I_m(1-e^x)$, respectively. Based on this proposition, Duncan obtained the average values for the eddy current, magnetizing current, and secondary eddy loss, and derived a per phase model [7].

In Duncan's model, the series resistance reflecting the eddy loss appears in series with the magnetizing inductance. The eddy current loss at the entry and exit is, in principle, the same as the core loss. The core loss is normally represented by a parallel resistor to the magnetizing inductor [12]. Therefore, the eddy current loss of the secondary conductor must also be described by a parallel resistor. However, in Duncan's model, the eddy current loss is described by a series resistor.

An equivalent circuit model for an LIM with the end-effect is shown on Fig. 7. Following Duncan's model, the magnetizing inductance at zero speed is $L_{m0}(1 - f(Q))$, where L_{m0} is the magnetizing inductance at zero speed and $f(Q) = (1 - e^{-Q})/Q$.

We neglect the eddy current loss R_{eddy} for the sake of simplicity. However, the inclusion of the loss branch increases the complexity of the equation greatly, while the presence or absence of the loss branch does not cause any significant difference in the current dynamics, unless the LIM is moving at a very high speed. Note that only Duncan's magnetizing inductance model is utilized here, while the resistance R_{eddy} reflecting the eddy current loss is neglected.

B. Model of LIM

Fig. 7 is a dq equivalent circuit that reflects the effect of the dynamic longitude end effect, based on Duncan's per phase equivalent model [7], [8].

In the equivalent circuit dq for end effect inclusion in Duncan's model, the magnetizing inductance is modified to $L_m 0(1 - f(Q))$, where Lm is the magnetizing inductance at zero speed and $f(Q) = (1-e^{-Q})$. A series resistance appears

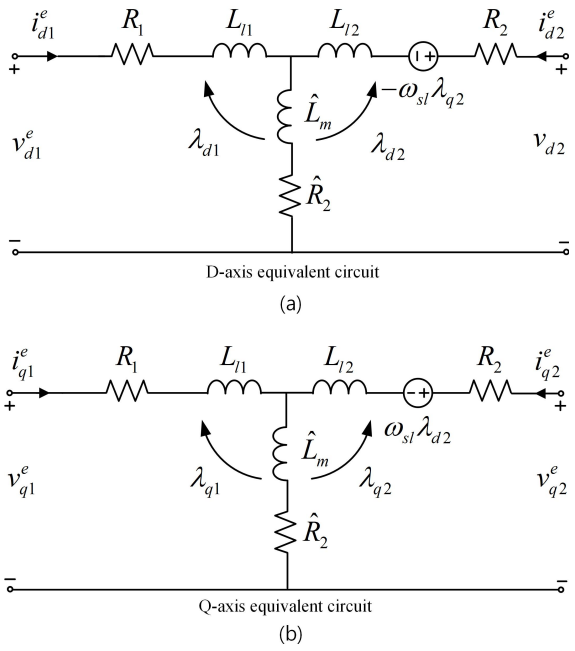

Fig. 7. d-q equivalent circuit of the LIM including the end effect in a stationary reference frame($\omega_{sl} = \omega_e - \omega_r$)

in the series with the magnetizing inductance, which reflects the eddy current loss due to the end effect and is equal to $R_r^{'} f(Q)$.

$$v_{d1} = R_1 i_{d1} + p\hat{\lambda}_{d1} - \omega_e \lambda_{q1} + \hat{r}_2 i_m \tag{3}$$
$$v_{q1} = R_1 i_{q1} + p\lambda_{q1} + \omega_e \hat{\lambda}_{d1} \tag{4}$$
$$v_{d2} = R_2 i_{d2} + p\hat{\lambda}_{d2} - \omega_{sl} \lambda_{q2} + \hat{r}_2 i_m \tag{5}$$
$$v_{q2} = R_2 i_{q2} + p\lambda_{q2} + \omega_{sl} \hat{\lambda}_{d2} \tag{6}$$

where $(v^e_{d1(d2)}, v^e_{q1(q2)})$, $(i^e_{d1(d2)}, i^e_{q1(q2)})$,$(\lambda^e_{d1(d2)}, \lambda^e_{q1(q2)})$ are the q-d axis voltage, current, and flux linkages of the primary(secondary) frame. ω_r denotes the secondary angular speed. The superscript e denotes the value in the synchronous reference frame.

$$\lambda^e_{q1} = L_{l1} i^e_{q1} + L_m\{1 - f(Q)\}(i^e_{q1} + i^e_{q2}) \tag{7}$$
$$\lambda^e_{d1} = L_{l1} i^e_{d1} + L_m\{1 - f(Q)\}(i^e_{d1} + i^e_{d2}) \tag{8}$$
$$\lambda^e_{q2} = L^{'}_{l2} i^e_{q2} + L_m\{1 - f(Q)\}(i^e_{q1} + i^e_{q2}) \tag{9}$$
$$\lambda^e_{q2} = L^{'}_{l2} i^e_{d2} + L_m\{1 - f(Q)\}(i^e_{d1} + i^e_{d2}) \tag{10}$$

The derived q-d dynamic equivalent circuit of the LIM in the stationary reference frame ($\omega_e = 0$) is represented in Fig.[]. Note that if $v_2 0$ 0, then $f(Q) \approx 0$, and if the LIM velocity $v_2 \to \infty$ as $f(Q) \to 1$. Therefore, the magnetizing inductance decreases as the speed increases due to the end effect.

The thrust developed by the machine is obtained by considering the power entering the two sources in the circuit diagram. The total mechanical power developed by the LIM is given by

$$p_{mech} = \frac{3}{2}\omega_r L_m\{1 - f(Q)\}(i^e_{q1}i^e_{d2} - i^e_{d1}i^e_{q2}) \tag{11}$$

where P_{mech} denotes the conversion of the electromechanical output power from electrical form to mechanical form. The mechanical LIM speed can be written as

$$\omega_2 = \frac{\pi}{\tau}V_2 \tag{12}$$

where τ denotes the motor pole pitch, and ω_2 denotes the electrical angular frequency, i.e., $\omega_2 = (P/2)\omega_m$. Thus, using (16), the developed thrust of LIM can be written as

$$F = \frac{P_{mech}}{V_2} = \frac{P_{mech}}{(\tau/\pi)\omega_2} \tag{13}$$

By substituting (12) into (13), the thrust can be expressed as

$$F = \frac{3}{2}\frac{\pi}{\tau}\{1 - f(Q)\}(i^e_{q1}i^e_{d2} - i^e_{d1}i^e_{q2}) \tag{14}$$

Note that unlike the torque equation in RIM, the $P/2$ gain in an LIM does not appear in the force equation because it is occult in the π/τ gain of the thrust.

IV. Simulation & Experiment for a High Efficiency Maglev

A. Analysis Model and Verification Conditions

Maglev trains consist of two cars per train. Each no-load vehicle weighs 26.5 tons and has a maximum acceleration and speed of 4 km/h/s, and 110 km/h, respectively. They have four bogies per vehicle, with two LIMs per bogies, and the maximum thrust per motor should be approximately 3.6 kN. Detailed vehicle specifications are shown in Table I.

When analyzing the energy consumption according to the change in the slip pattern, it is desirable to perform the analysis based on the traveling pattern, including acceleration, deceleration, and coasting. Therefore, the "test area" of Fig. 3 is simulated and compared with the fixed and variable slip control methods. The power measurements of the fixed and variable slip operations were compared and analyzed with the power measuring equipment installed in the actual vehicle.

B. Simulation for Maglev Train

Fig. 8 shows the waveforms simulated according to the actual driving pattern. Driving was performed for 75 s and the case with the most common driving pattern was selected and simulated. Simulation results show that the energy consumption is 0.761 kWh for the conventional slip frequency operation. The variable slip frequency operation consumed 0.615 kWh, which was 20% lower than that of the constant slip frequency operation with the same operation performance.

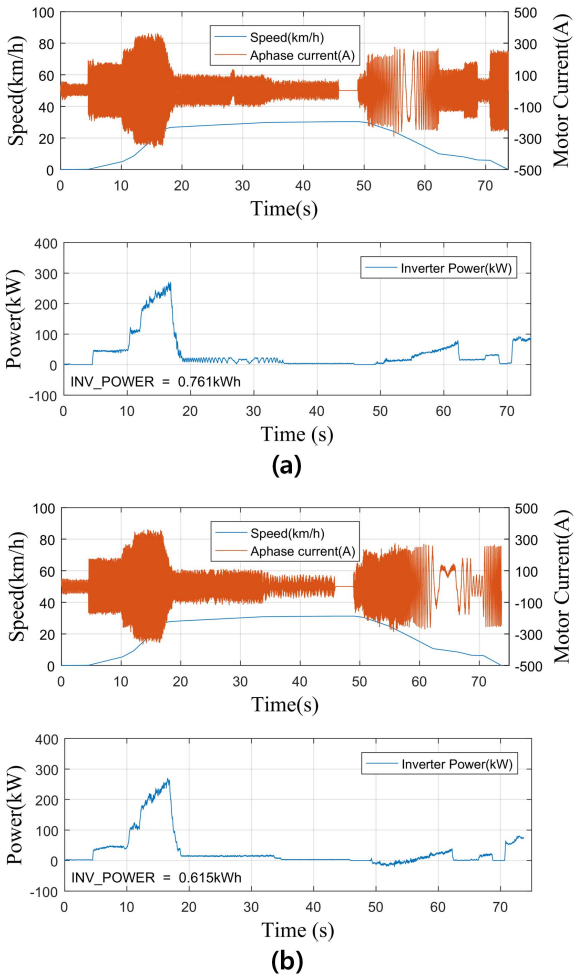

Fig. 8. Maglev running simulation waveform (a) Constant slip pattern driving, (b) Proposed slip pattern driving

C. Experiment for Maglev Train

Fig. 9 is the experimental waveform actually performed on the Korean Maglev train. (a) is a waveform that was operated at the conventional 12.5 Hz slip frequency, and (b) is an experimental waveform that was operated by changing the slip according to the current command. In fig. 9 (a) with constant slip frequency, the inverter power of the propulsion system is 1.032 kWh, and the levitation system consumes 0.294 kWh. In fig. 9 (b) with variable slip frequency, the inverter power is 0.775 kWh and the levitation system consumes 0.293 kWh. It was confirmed that the levitation system consumes almost the same power regardless of the slip pattern, and the propulsion system can confirm that the power consumption is reduced by 24%.

V. Conclusion

In this study, the efficiency of the LIM is analyzed using the propulsion system of a maglev train; the system exhibits the highest energy consumption rate. Because the efficiency of the LIM increases with a decrease in the slip frequency,

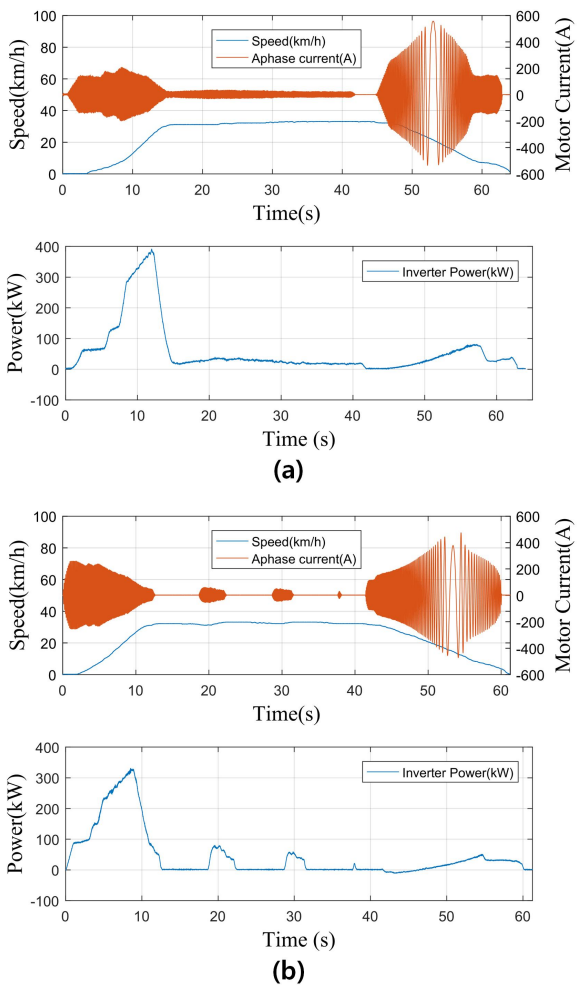

Fig. 9. Maglev running experiment waveform (a) Constant slip patterns driving, (b) Proposed slip patterns driving

an operation method that varies the slip frequency according to the thrust is proposed. The proposed method and previously used constant slip frequency method were applied to a real train. The test results confirmed that the proposed slip frequency modification technique does not affect the injury and reduces the energy consumption by 24%. In this study, a method for improving the efficiency of a LIM used in maglev trains is analyzed. We could confirm that to the proposed method helped improve the performance of real trains.

REFERENCES

[1] H. S. Han and D. S. Kim, *Magnetic Levitation*. Netherlands: Springer, 2016.

[2] B. T. Ooi and D. White, "Traction and Normal Forces in the Linear Induction Motor," *IEEE Transactions on Power Apparatus and Systems*, vol. PAS-89, no. 4, pp. 638–645, apr 1970.

[3] H. Seo, J. Lim, G.-H. Choe, J.-Y. Choi, and J.-H. Jeong, "Algorithm of Linear Induction Motor Control for Low Normal Force of Magnetic Levitation Train Propulsion System," *IEEE Transactions on Magnetics*, vol. PP, pp. 1–4, 2018.

[4] J. Lim, D.-Y. Park, and J.-H. Jeong, "A Study on Optimal Operating Point of Linear Induction Motor Considering Normal Force and Efficiency in MAGLEV Vehicle," *IEEE Transactions on Magnetics*, pp. 1–5, 2018.

[5] I. Boldea, *Linear Electric Motors, Englewood Cliffs," NJ*. USA: Prectice-Hall, 2001.

[6] G. Kang and K. Nam, "Field-oriented control scheme for linear induction motor with the end effect," *IEE Proceedings - Electric Power Applications*, vol. 152, no. 6, pp. 1565–1572, 2005.

[7] J. Duncan, "Linear induction motor-equivalent circuit model," *IEE Proc. Electr. Power Appl.*, vol. 130, pp. 51–57, june 1983.

[8] P. Hamedani and A. Shoulaie, "Indirect field oriented control of linear induction motors considering the end effects supplied from a cascaded H-bridge inverter with multiband hystersis modulation," in *PEDSTC 2013 - 4th Annual International Power Electronics, Drive Systems and Technologies Conference*. IEEE, feb 2013, pp. 13–19.